PHILOSOPHICAL MAGAZINE, 2003, VOL. 83, NO. 6, 727–743
Taylor & Francis
Taylor & Francis Group

Competitive segregation of gallium and indium at heterophase Cu–MnO interfaces studied with transmission electron microscopy

S. MOGCK, B. J. KOOI and J. TH. M. DE HOSSON†

Department of Applied Physics, Materials Science Centre and Netherlands Institute of Metals Research, University of Groningen, Nijenborgh 4, 9747 AG Groningen, The Netherlands

[*Received 10 May 2002 and accepted in revised form 28 September 2002*]

ABSTRACT

This paper concentrates on the possible segregation of indium and gallium and competitive segregation of gallium and indium at atomically flat parallel {111}-oriented Cu–MnO interfaces. The segregation of gallium at Cu–MnO interfaces after introduction of gallium in the copper matrix of internally oxidized Cu–1 at.% Mn could be hardly detected with energy-dispersive spectrometry in a field emission gun transmission electron microscope. After a heat treatment to dissolve indium in the copper matrix, gallium has a weak tendency to segregate, that is 2.5 at.% Ga per monolayer at the interface compared with 2 at.% in the copper matrix. The striking result is that this gallium segregation is observable because it does not occur at the metal side of the interface but in the first two monolayers at the oxide side. Using the same heat treatment as for introducing indium in the sample, but without indium present, gallium segregates strongly at the oxide side of the Cu–MnO interface with a concentration of about 14.3 at.% in each monolayer of the two. In contrast, the presence of gallium has no influence on the segregation of indium towards Cu–MnO interfaces, because the outermost monolayer at the metal side of the interface contains 17.6 at.% In, that is similar to previously found results. This leads to the intriguing conclusions, firstly, that, in contrast with antimony and indium, gallium segregates at the oxide side of the interface and, secondly, that the presence of indium strongly hampers gallium segregation. The results from analytical transmission electron microscopy on gallium segregation are supported by high-resolution transmission electron microscopy observations.

§1. INTRODUCTION

In most materials, impurity or alloying elements are present which can segregate to grain boundaries or heterophase interfaces. Segregation of such elements may influence many important material properties (Johnson *et al.* 1979). In contrast with homophase interfaces, detailed studies of segregation at *heterophase* interfaces have been only scarcely reported (Hayes and Grieveson 1995, Shashkov 1997), partly because of experimental difficulties in detecting small amounts of a solute material at atomic planes. Recently, appropriate techniques became sufficiently sophisticated to allow chemical analysis of heterointerfaces near or on the atomic scale (Rühle 1997,

† Email: hossonj@phys.rug.nl.

Philosophical Magazine ISSN 1478–6435 print/ISSN 1478–6443 online
http://www.tandf.co.uk/journals
DOI: 10.1080/0141861021000049238

Shashkov 1997, Shashkov *et al.* 1999, Pipel *et al.* 2000, Sebastian *et al.* 2001, Vriesendorp *et al.* 2001), for example (scanning) transmission electron microscopy ((S)TEM) combined with X-ray energy-dispersive spectrometry (XEDS) or parallel electron-energy-loss spectroscopy (PEELS) and high-angle annular dark-field (*Z*-contrast) detection.

Nowadays three methods are available to reveal segregation at interfaces using analytical (S)TEM at edge-on oriented interfaces in a TEM foil:

(i) taking a line scan;
(ii) chemical mapping;
(iii) using a scan raster.

A drawback of line scans and maps is related to drift of the sample and/or the electron beam. The sample drift may occur because of local heating by the electron beam and cannot be fully eliminated. Both kinds of drift are harmful for a detailed analysis because, in order to detect small enrichments in just one monolayer, the steps between measurement points have to be made small and the detection time per point has to be made sufficiently large to record significant signals. A line scan is in general statistically inadequate for analysing strong concentration gradients at interfaces, because of the lack of a sufficient number of spots in the crucial region. In (S)TEM mode the concentrations measured are not the actual values but are convoluted spatially with the electron probe. In the case where the size of the fluctuations in concentration is smaller than the probe size (for instance an enrichment in only 1 monolayer with a thickness of 0.2 nm whereas the effective probe size is for instance 1 nm) the measured concentration depends sensitively on the *exact* position of the electron probe with respect to the concentration fluctuation. Using a line scan or elemental mapping the position of the probe is in general not known accurately enough to obtain the actual concentrations, that is to perform the deconvolution. A scan raster overcomes these problems of drift and inadequacy, but at the expense of a decrease in detection sensitivity due to averaging over a larger volume. Another way to circumvent this problem without losing detection sensitivity is offered by our novel approach as has been delineated by Kooi *et al.* (2002). It should be stressed, however, that this methodology is specifically applicable to heterophase interfaces. The basic idea is that the measured solute concentration is plotted against one of the two measured solvent concentrations showing an abrupt concentration change at the interface and fitted with theoretical curves based on assumed concentration profiles that are convoluted with a (Gaussian) function mimicking the electron probe. For more details of this approach and discussion in comparison with the other approaches reference should be made to the paper by Kooi *et al.* (2002).

In this paper we apply this methodology to a study of the possible segregation of gallium and indium at parallel {111}-oriented Cu–MnO interfaces, with particular emphasis on the competitive segregation behaviour between gallium and indium. The analytical TEM results will be combined with high-resolution transmission electron microscopy (HRTEM) observations in order to study the gallium segregation behaviour.

§ 2. Experimental details

An alloy containing copper with 1 at.% Mn was made in a high-frequency furnace by melting the pure constituents (99.99% by weight) in an alumina crucible under a protective atmosphere of oxygen-free argon. Ingots were homogenized

(1 week at 700°C in an evacuated quartz tube) and subsequently cold rolled from 4 mm down to 0.5 mm. The Cu–MnO interfaces were obtained by internal oxidation for 17 h at 900°C using the pack technique of Rhines and Grobe (1942); that is, an envelope of copper foil was filled with the sample and Cu, Cu_2O and Al_2O_3 powder in a volume ratio of about 1 : 1 : 1 and was placed in an evacuated quartz tube. Internal oxidation of Cu–1 at.% Mn yields octahedrally shaped MnO precipitates with a cube-on-cube orientation relation with the copper matrix. The MnO precipitates have a NaCl-type crystal structure and the average size of the oxide particles is 200 nm. A large mismatch of 22.9% is present at the {111} planes forming the interfaces between Cu and MnO, which leads to the formation of semi-coherent interfaces. Further details of MnO precipitates in copper matrix have been extensively described by Kooi *et al.* (1998), De Hosson *et al.* (1999) and Groen *et al.* (1999).

After internal oxidation, approximately 3.5 at.% Ga was placed together with the sample, without making mutual contact, inside an evacuated quartz tube for 1 week at 700°C. After 1 week, nearly all gallium is dissolved more or less homogeneously in the copper matrix. Next, two different treatments were used. One consisted of introducing approximately 3.5 at.% In in the copper matrix using the same treatment as for gallium, that is 1 week at 750°C. The other consisted of the same annealing treatment but without indium present.

TEM samples were prepared by grinding, dimpling and ion milling (using liquid-nitrogen cooling) 3 mm discs to electron transparency. The XEDS measurements were carried out using a JEOL 2010F, field emission gun transmission electron microscope operating at 200 kV and equipped with an EDAX X-ray energy-dispersive spectrometer with a super-ultrathin window. A double-tilt beryllium sample holder was used. The measurements were performed with an electron probe diameter characterized by a full width at half-maximum (FWHM) of 0.7 nm. During the XEDS measurements the samples were oriented in the ⟨110⟩ copper matrix orientation, to ensure that the electron beam is edge on to {111}-oriented Cu–MnO planar interfaces. The sample was always tilted towards the detector over an angle between 10 and 30°. The dead time was never larger than 40% and never smaller than 10%. This was achieved by using time constants varying between 35 and 100 μs, corresponding to an energy resolution relative to Mn Kα varying from 135 to 145 eV respectively. After a manual background subtraction, quantification of X-ray energy-dispersive spectra was carried out using the Cliff–Lorimer (1975) ratio technique in the thin-film approximation:

$$\frac{C_A}{C_B} = k_{AB}\frac{I_A}{I_B},$$

where C_A and C_B are the concentration of elements A and B respectively in the specimen, I_A and I_B are the measured intensities in the X-ray spectrum and k_{AB} is the Cliff–Lorimer factor. For the quantification of the compositions the theoretical Zaluzec k_{AB} factors were used (EDAX 2000). In the analysis of segregation we are primarily interested in the relative enrichment at the interface compared with the bulk and therefore the use of (in an absolute sense) less accurate theoretical k_{AB} factors is justified. For the determination of the composition across an interface a large number of spectra were obtained by positioning the beam for 40 s on the interface and subsequently shifting the beam (manually using the deflection coils) to other parts of the interface. These measurements were completed by a limited

number of spectra from areas close to the interface on both sides of the interface. After quantification the indium and gallium concentrations were related to the copper concentration and compared with the model description as explained by Kooi *et al.* (2002). This model description is based on assumed concentration profiles that are of simple nature; for instance the atomic fraction of gallium or indium in the copper matrix has a value x (that of copper has a value $1 - x$), in the outermost monolayer of the metal at the interface has a value y (that of copper has a value $1 - y$) and the concentrations of gallium or indium and copper are zero in the oxide. These concentration profiles are convoluted with a Gaussian function mimicking the electron probe. Note that the FWHM characterizing the probe size incorporates beam broadening. For instance the initial FWHM of the probe entering the sample surface is 1 nm and at the exit plane of TEM sample is 2 nm. The average thickness of the sample region studied was 50 nm. Then we assume the effective probe size to be 1.5 nm (FWHM).

High-resolution transmission electron micrographs were recorded in a JEOL 4000EX/II, operating at 400 kV (spherical aberration coefficient, 0.97 ± 0.02 mm; defocus spread, 7.8 ± 1.4 nm; beam semiconvergence angle, 0.9 mrad). HRTEM images were obtained by digitizing negatives using a charge-coupled device camera and the grey scale was adapted to achieve reasonable brightness and contrast. HRTEM images were not filtered.

§ 3. Results and discussion

3.1. *Energy-dispersive spectroscopy analyses*

TEM samples with MnO precipitates in copper were analysed after the three different segregation treatments. In the first sample only gallium was introduced (1 week at 700°C). In the second sample, after the gallium treatment, indium was also dissolved (an additional week at 750°C). The third sample was, after the gallium treatment, subjected to the same heat treatment as for introducing indium, but without indium present. XEDS results for these three cases for the copper matrix and the MnO precipitates are presented in table 1. The errors of the measured concentrations are based on an average over five spectra (Gaussian statistics). An additional systematic error is introduced by the theoretical k_{AB} factors. The measured oxygen concentration in the copper matrix and the small amounts of copper found during the measurement in the MnO precipitates can be assigned to spurious X-rays, because all these measurements were taken near the interfaces. From this point of view it becomes clear that no indium and gallium are dissolved in the MnO

Table 1. XEDS results for the copper matrix and MnO precipitates (average of five spectra).

	Cu	*Mn*	*O*	*Ga*	*In*
Cu 1 at.% Mn 3.8 at.% Ga (just after introduction of Ga)					
Copper matrix	93.6 ± 1.2	0.5 ± 0.4	2.2 ± 1	3.8 ± 0.4	–
Cu 1 at.% Mn 3.8 at.% Ga 3.4 at.% In (after introduction of In at 750°C for 1 week)					
Copper bulk	91.8 ± 1.3	0.4 ± 0.2	2.5 ± 1.3	2.0 ± 0.3	3.4 ± 0.4
MnO precipitate	5.7 ± 1.2	51.6 ± 7.6	42.2 ± 7.1	0.2 ± 0.1	0.2 ± 0.2
Cu 1 at.% Mn 3.8 at.% Ga (after annealing at 750°C for 1 week)					
Copper matrix	92.4 ± 1.7	0.7 ± 0.5	5.1 ± 1.7	1.9 ± 0.3	–

precipitates. Measurements to analyse the possible segregation of indium and gallium were repeated for three different interfaces in each sample and all three measurements showed similar segregation behaviours.

Figure 1 displays the results of the model calculations for segregation at a metal–oxide interface where the matrix is not detectably present in the oxide. The concentration of the segregant is plotted versus the metal concentration. In all cases the segregant is dissolved in the metal matrix with a concentration of 3.1 at.% and it is not detectably present in the oxide. The solid curves are for concentrations of 10 and 20 at.% segregant in the outermost monolayer of the metal and the broken curves for concentration of 10 and 20 at.% segregant in the first monolayer of the oxide The probe is represented by a Gaussian function with a FWHM of 0.7 nm.

The results show that in principle it is possible to distinguish where the enrichment is localized. For segregation at the oxide side of the interface the maximum of the segregant concentration shifts to a lower metal concentration than expected for segregation at the metal side of the interface. Below it will be demonstrated that gallium has a tendency to segregate at the oxide side of the interface, as opposed to indium that tends to segregate at the metal side of the interface.

Figure 2 shows the gallium concentration across a {111}-oriented Cu–MnO interface just after the introduction of gallium into the internally oxidized Cu–1 at.% Mn. There is hardly any segregation of gallium recognizable. Thus, all the measured gallium concentrations versus the copper concentration across the interface can be described with a straight line. The fitting procedure (see for more details appendix A) assuming an effective probe size (FWHM) of 1.4 nm already indicates a gallium concentration of 1.8 at.% per monolayer in the first two monolayers of the oxide. The reason why we assume that the gallium is in the first two monolayers of

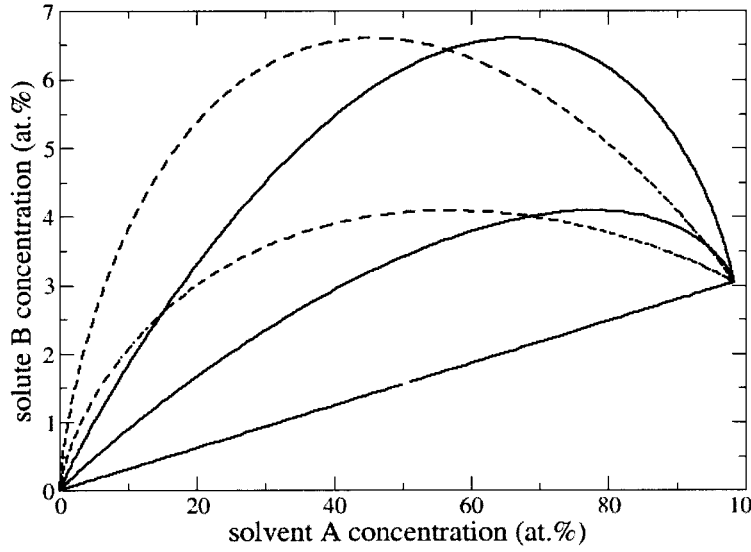

Figure 1. The concentration of segregant B plotted versus the concentration of the metal A (only present at one side of the A–C heterointerface) for B concentrations of 10% and 20% in the outermost metal monolayer (solid curves) and in the first monolayer of the oxide (broken curves) at the interface. The probe size is 0.7 nm (FWHM of a Gaussian function).

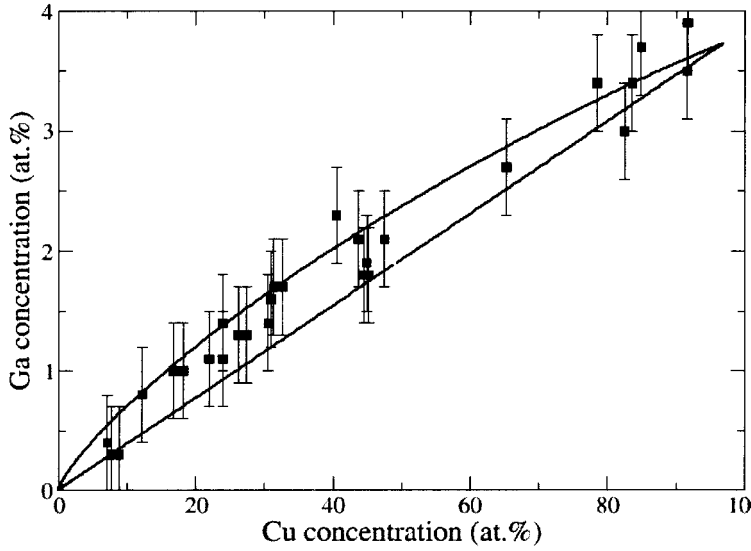

Figure 2. After gallium dissolution at 700°C for 1 week into internally oxidized Cu–1 at.% Mn, about 3.8 at.% Ga is dissolved in the copper matrix. The almost straight line indicates that gallium does not significantly segregate at the interface.

the oxide will be discussed later. Note that the gallium concentration in the copper matrix is 3.8 ± 0.4 at.% (homogeneous).

After 1 week at 750°C for the intake of indium, segregation of gallium is rather limited but already unambiguously detected. Only a small concentration of 2.5 at.% per monolayer is present in the first two monolayers of the oxide side of the interface (figure 3).

Already at this stage the fitting procedure clearly indicates that the data are better fitted with a concentration profile that assumes the gallium to be in the first monolayer or the first two monolayers of the oxide instead of the outermost monolayer of the metal matrix. Note that now the gallium concentration in the copper matrix has dropped to 1.9 ± 0.3 at.%. Thus, it appears that during the heat treatment and the dissolution of indium the gallium concentration at the interface obtains more or less the value that was originally present in the copper matrix. In the copper matrix itself the concentration of gallium decreases owing to the segregation of gallium at grain boundaries and owing to the formation of spinel-type $Ga_xMn_yO_4$ precipitates (see also the next section).

After the dissolution of indium, the segregation of indium occurs at the Cu–MnO interfaces as shown in figure 4. The presence of indium and gallium in Cu–1 at.% Mn results in an indium segregation of approximately 17 at.% in the terminating copper monolayer at the parallel {111}-oriented Cu–MnO interface, whereas the average indium concentration in the copper matrix was only 2.9 at.% (see figure 4). The indium segregation of 17.6 at.% in the terminating monolayer is very similar to previous measurements of indium segregation of 15 at.% without the presence of gallium at the Cu–MnO interface (see also Kooi *et al.* (2002)). Apparently, there is no influence of the presence of gallium on the indium segregation to {111}-oriented Cu–MnO interfaces.

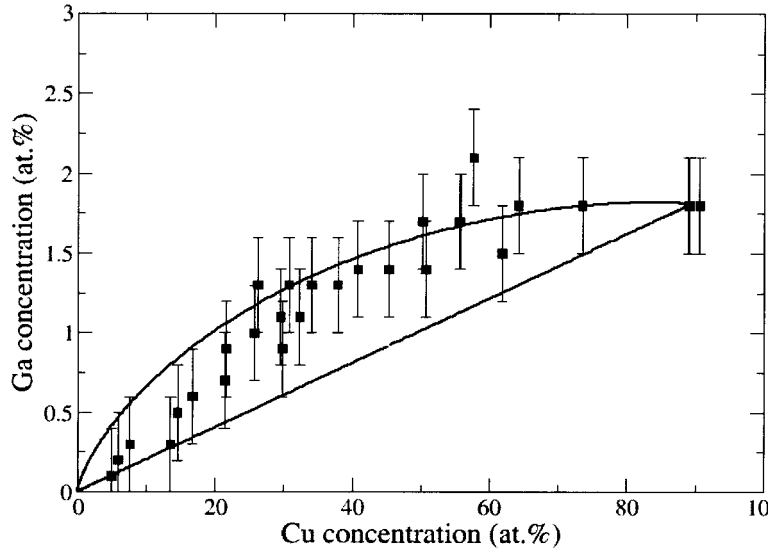

Figure 3. XEDS results together with the model curve. The curve holds for a gallium concentration in the copper matrix of 2 at.% and a probe size of 1.4 nm. The best match of the model curve with the XEDS measurement is reached with a gallium concentration of 2.5 at.% in the first two MnO monolayers at the Cu–MnO interface.

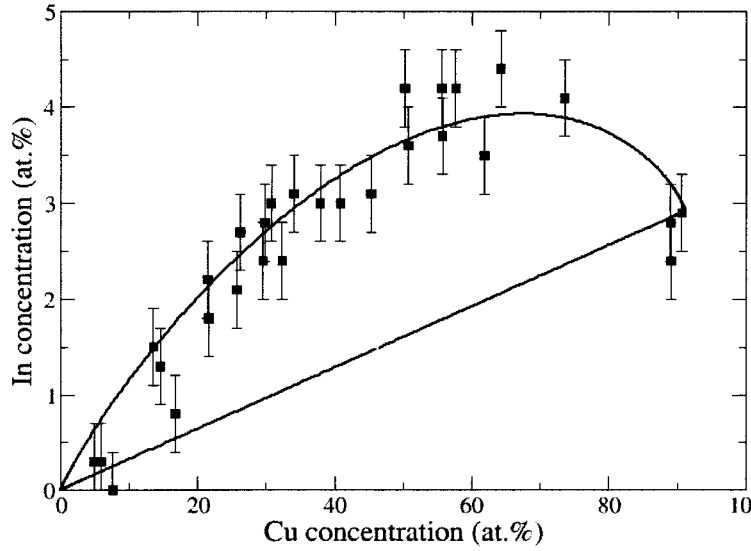

Figure 4. XEDS results together with the model curve. The curve holds for an indium concentration in the copper matrix of 3.0 at.% and a probe size of 1.4 nm. The best match of the model curve with the XEDS measurement is reached with an indium concentration of 17.6 at.% in the outermost copper monolayer at the Cu–MnO interface.

In order to investigate the influence of gallium segregation without the presence of indium, heat treatment of Cu–1 at.% Mn–3.8 at.% Ga at 750°C for 1 week *in vacuo* was performed. Heat treatment without the presence of indium appears to result in significantly higher gallium segregation, as shown in figure 5. The theoretical curve in figure 5 holds for a layer 0.4 nm (2 monolayers) thick at the oxide side of the interface with a gallium concentration of 14.3 at.% per monolayer and a gallium concentration in the matrix of 2.0 at.%. From the fitted data in figure 5 it becomes apparent that the gallium segregation takes place at the oxide side of the interface and with the information obtained from HRTEM images a thickness of 2 monolayers appears to be consistent with this. The concentration of 14.3 at.% Ga may indicate that gallium and MnO are locally transformed into $GaMn_2O_4$. Thus, without the presence of indium, gallium segregates strongly at the oxide side of the interface and, with indium present, gallium shows only weak signs of segregation. These results show unambiguously that indium segregation at the Cu–MnO interface seals the first monolayers at the oxide side of the boundary for the segregation of gallium.

Using our fitting procedure to the data shown in figures 2–5 revealed that in the case of gallium the fitting was always better if the gallium was assumed to be in the first 2 monolayers of the oxide than in the outermost monolayer of the metal matrix, whereas for indium the opposite was clearly indicated.

All the measurements were made using an electron probe that initially has an estimated size of 0.7 nm FWHM. Using the smaller 0.5 nm probe size the count rate is too low when an interface close to the hole in the TEM specimen is studied and an interface in a thicker region has to be found. On the other hand the beam broadening inside the specimen has to be taken into account and varies with the thickness to the

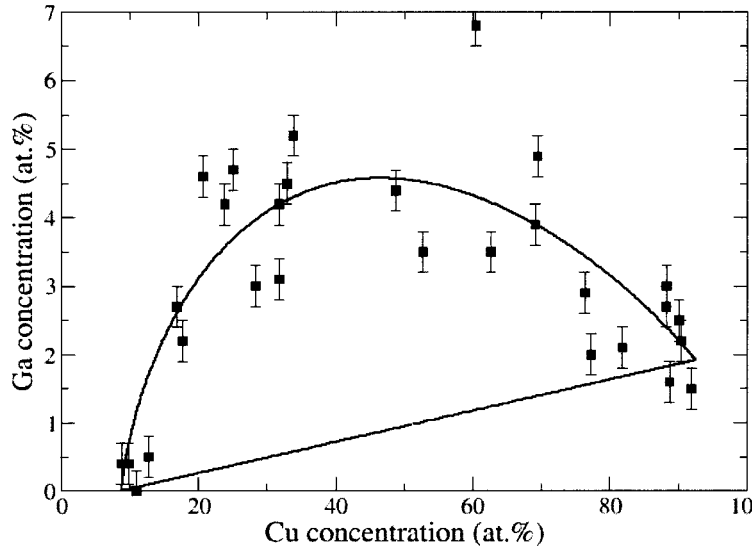

Figure 5. XEDS results together with the model curve. The curve holds for a gallium concentration in the copper matrix of 2.0 at.% and a probe size of 1.4 nm. The best match of the model curve with the XEDS measurement is reached with a gallium concentration of 14.3 at.% in the first two monolayers at the oxide side of the Cu–MnO interface.

power of 3/2 (Reed 1982). The best interfaces are found in thin areas relatively close to the hole in the specimen. A compromise has to be found between a sufficient count rate and the beam broadening. For the probe size used to generate the model curves in figures 2–5 a FWHM of 1.4 nm was estimated which *includes* the beam broadening in the sample. The procedure to include the beam broadening in an effective probe size is fairly accurate, although it is rather difficult to make an accurate estimate of this effective probe size. Therefore the results of our fitting procedure, for instance the 17.6 at.% In in the outermost monolayer of the copper matrix, suggests an accuracy that is actually not present, because owing to possible variations in probe sizes the relative error is probably of the order of 30%. Consequently a more realistic value for the indium concentration in the outermost layer of copper is 17.6 ± 5 at.%. Of course, there are practical solutions to determine the final probe size better but at least knowledge of the drift for each data point is then necessary.

From the energy-dispersive spectrometry (EDS) measurement it is clear that a higher extent of segregation at heterophase interfaces results in a larger scatter among the values for the measured concentrations, especially near the maximum of the model curves. The major reason for this scatter is the drift of the sample (or electron beam) during the 40 s used to record a spectrum. The effect of drift can in principle be incorporated in the effective probe size of each individual measurement. Using the modelled curves it is assumed that the probe size is a constant for all measurement points. In practice this will not be the case and in fact the different data points correspond to curves with different effective probe sizes (cf. figure 2 (*b*) in the paper by Kooi *et al.* (2002)). Only in the case of segregation do these different effective probe sizes matter, because a straight line in the case of the absence of any segregation remains also a straight line independent of the probe size. A clear example of this is shown in figure 6. It holds, because segregation of Zn at the Cu–

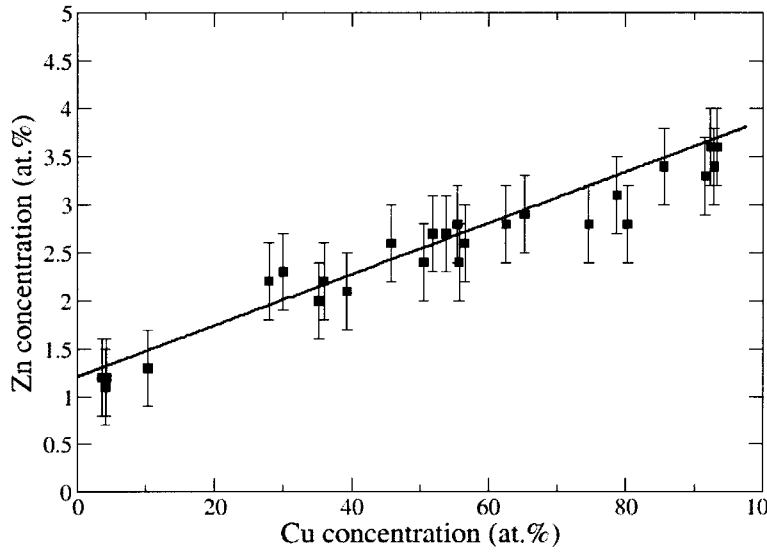

Figure 6. EDS results of zinc concentrations across a Cu–MnO interface. It indicates clearly that zinc does not segregate to the interface. However, about 1.2 at.% Zn is dissolved in the MnO precipitate. The measurement was performed with a FWHM probe size of 0.7 nm.

MnO interfaces does not occur. The measured zinc concentration does not show any significant scatter with respect to the straight line. All error bars in the plots of the XEDS measurements in figures 2–6 are related to the typical errors listed in table 1.

3.2. *High-resolution transmission electron microscopy observations*

EDS, selected-area electron diffraction patterns and HRTEM showed that in all samples the MnO precipitates are in the minority, because about a half to two thirds of the precipitates have a spinel-type structure and a composition corresponding to $Ga_xMn_yO_4$ with x varying between 1 and 2 and y between 2 and 1 (as we determined using EDS) and only the remainder is MnO. All results analysed up to this stage hold for the MnO precipitates. An example of a spinel precipitate in copper is shown in the HRTEM image in figure 7. A cube-on-cube orientation relation holds between

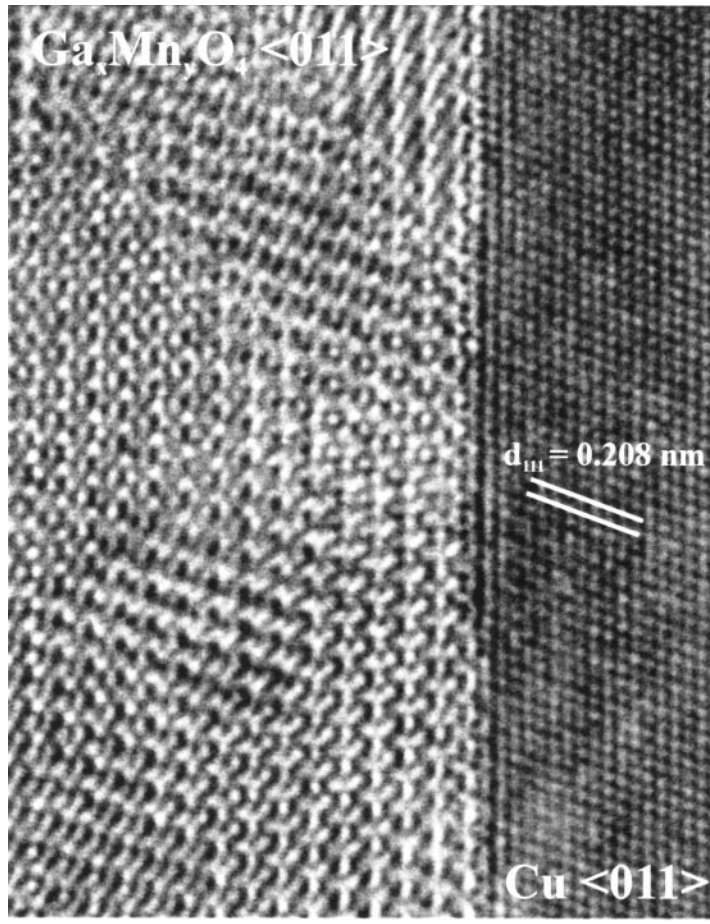

Figure 7. HRTEM image of parallel {111} interface between copper and the spinel $Ga_xMn_yO_4$ (where x could vary between 1 and 2 and y between 2 and 1) as viewed along a common ⟨011⟩ of copper and spinel. In the sample, gallium was dissolved by annealing for 1 week at 700°C during which the gallium reacted with the MnO and formed the spinel. Finally, about half to two thirds of all precipitates became spinel and the rest remained MnO.

the spinel and the copper and the precipitates have octahedral shapes owing to the dominant {111} facets. The oxygen sublattices of the spinel and MnO are identical; only the distributions of the cations over the interstitial sites in the O sublattice differ for the two phases. Analysis of the misfit between the copper and spinel indicates that the lattice constant of the spinel is 2×1.176 the lattice constant of copper (the fcc oxygen sublattce of the spinel is measured 1.176 times larger than the fcc copper lattice and the factor 2 arises because the unit cell of spinel is twice the fcc unit cell when considering the oxygen sublattice only); that is, using 0.3615 nm for copper this gives 0.850 nm for the spinel. This value is very close to 0.846 nm that holds for the lattice constant of the known spinel Ga_2MnO_4 (Joint Committee for Powder Diffraction Standards 1992).

The presence of $Ga_xMn_yO_4$ precipitates indicates that gallium has a tendency to react with the MnO to form a new phase. Therefore it is not completely surprising that gallium in MnO precipitates has a tendency to segregate to the oxide side of the interface. However, this is not a general rule, because for instance zinc has also a strong tendency to react with MnO to give spinel-type $Zn_xMn_yO_4$ precipitates, but it does not segregate at all at Cu–MnO interfaces, at the oxide side nor at the metal side (see, for example, figure 6). A distinct difference between zinc and gallium is that the former is partially soluble in MnO, as can be seen from the 1.2 at.% Zn that is already homogeneously distributed in the MnO precipitate in figure 6, whereas gallium does not appear soluble in the MnO but has to nucleate the spinel phase. Hence, the interface does not appear to form a barrier where enrichment occurs for zinc, whereas it does for gallium.

A HRTEM image of a Cu–MnO interface is shown in figure 8 for a sample in which gallium was dissolved (1 week at 700°C) and which was annealed for an additional week *in vacuo* at 750°C. The Cu–MnO interfaces are constituted by {111} planes and viewed along their common ⟨011⟩ direction. A thin layer, appearing less well ordered than the MnO and copper and positioned in between the MnO and the copper is clearly visible in figure 8. The thickness of the layer is approximately 0.5 nm.

The EDS measurements revealed for this case a high gallium concentration at the oxide side of the interface. Although not clearly visible, the HRTEM image indicates, based on mismatch between the thin layer and either the MnO or the Cu, that the thin layer is more intimately connected to the oxide than to the metal part. Based on mismatch it forms an intermediate between the MnO and copper, which have a large misfit of 22.9%. The misfit of the intermediate layer is smaller with the MnO than with the copper. Probably the phase in this intermediate layer is related to the above-mentioned spinel precipitates and the spinel-type Ga_2MnO_4 (Joint Committee for Powder Diffraction Standards 1992). The lattice constant of this spinel is 0.846 nm, compared with 0.4444 nm for MnO and 0.3615 nm for copper. So, the misfit at the metal–oxide interface is reduced from 22.9% for Cu–MnO to 17.0 % for Cu–spinel, where we consider that the lattice constant of the fcc oxygen sublattice with half that of the spinel. However, based on the chemical composition (14.3 at.% Ga) it is more likely that the layer contains $GaMn_2O_4$ instead of Ga_2MnO_4.

A plausible explanation for the gallium segregation at the oxide side of the Cu–MnO interface is that a thin outer $Ga_xMn_yO_4$ layer around the MnO reduces the metal–oxide interfacial energy by reducing the mismatch energy at the interface. In principle, one sharp Cu–MnO interface is replaced by two interfaces with a thin

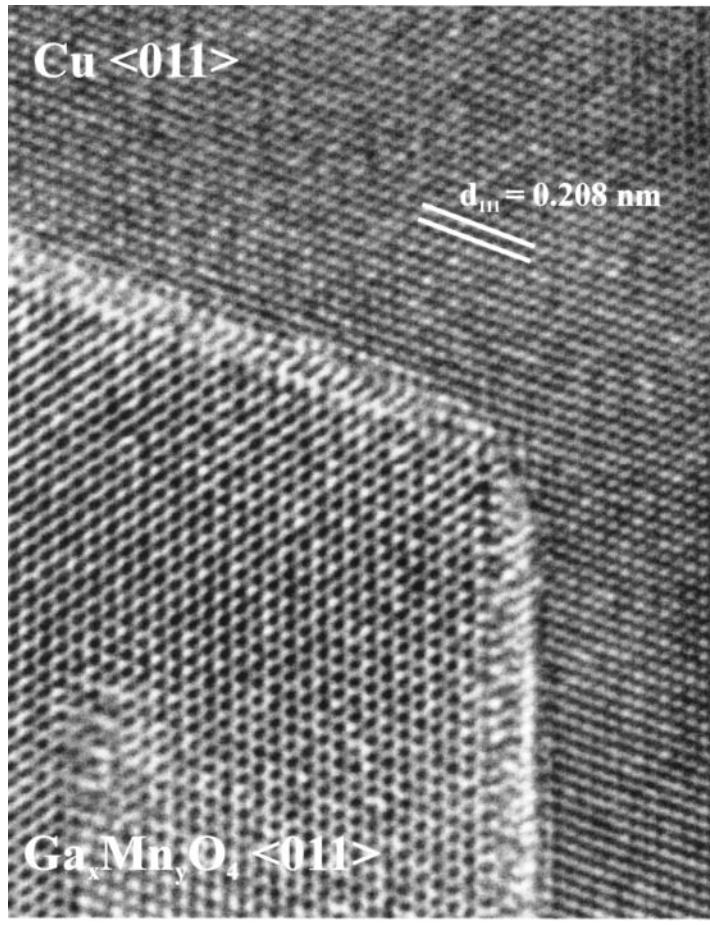

Figure 8. HRTEM image of parallel {111}-oriented Cu–MnO interfaces as viewed along a common ⟨011⟩ of copper and MnO. In the sample, gallium was dissolved by annealing for 1 week at 700°C and subsequently the sample was vacuum annealed for 1 week at 750°C. In between the copper and MnO a thin layer of $Ga_xMn_yO_4$ appears to be present with a thickness of about 0.5 nm that reduces the misfit at the Cu–MnO interface.

gradient layer in between. From a thermodynamic point of view it is probably favourable to get rid of the spinel–MnO interface and to transform the MnO fully into $Ga_xMn_yO_4$. However, in the system the total number of manganese and oxygen atoms is in principle fixed (in the evacuated quartz tube) and only gallium is supplied. Therefore the limiting factor for transformation of MnO into $Ga_xMn_yO_4$ is the amount of oxygen. Under this limiting oxygen condition it is impossible to transform the MnO fully, but still it appears possible to form a thin layer of $Ga_xMn_yO_4$ at the interface which can apparently reduce the interfacial energy.

The explanation for the indium segregation is straightforward. Indium atoms that segregate at the metal side of the Cu–MnO interface prefer the sites in between the misfit dislocation cores of the network at the interface, because these sites offer more space for the relatively large indium atoms than present in the copper matrix (Kooi *et al.* 2002). An explanation for the blocking effect of indium on the segrega-

tion of gallium to the oxide side of the interface is not as straightforward. There could be a kinetic reason: indium atoms are strongly fixed to the special sites at the interface that are also needed for the transport of gallium atoms from the copper matrix to the oxide precipitate or vice versa. In this way the gallium diffusion across the interface can be strongly hampered. However, there could also be a thermodynamic reason. It has to be kept in mind that annealing the Cu–MnO system *in vacuo* with gallium or indium vapour reduces strongly the oxygen partial pressure that the system is subjected to. After internal oxidation the system had a tendency to become in equilibrium with the oxygen partial pressure corresponding to the dissociation pressure of Cu_2O. However, after annealing in gallium or indium vapour the oxygen partial pressure is reduced to the dissociation pressure pertaining to gallium or indium oxide. After internal oxidation the terminating layer of MnO at the parallel {111}-oriented Cu–MnO interface will be a close packed oxygen plane, whereas after annealing in gallium or indium vapour the terminating layer of MnO will probably become a close-packed Mn plane (Mader 1992, Backhaus-Ricoult and Laurent 1999, Backhaus-Ricoult 2000, 2001). Gallium segregation at the oxide side of the interface thus implies that the terminating close-packed plane of the oxide will contain a large number of gallium atoms next to the manganese atoms. Indium segregation at the metal side of the interface thus would imply a large number of In—Ga bonds across the interface. If these bonds are not favourable, as appears the case considering the binary Ga–In phase diagram (Baker 1992), then the presence of indium can destabilize the presence of gallium atoms at the oxide side of the interface. On the other hand Cu—Ga bonds across the interface can be favourable (gallium is soluble in copper, even at low temperatures, and can form several intermetallic phases with copper (Baker 1992)). This can explain the observed results that, without the presence of indium, gallium segregates at the oxide side of the interface and, with the presence of indium, gallium segregation is hampered.

Another even less well understood but also intriguing observation was made concerning the dissolution of gallium in the Cu–MnO system. Vacuum annealing MnO precipitates in pure copper results in the usual tendency for clustering and Ostwald ripening of the MnO precipitates in order to decrease the total amount of interfacial energy. We have already reported in previous publications that antimony is able to suppress this clustering and Ostwald ripening, keeping the number and size of the MnO precipitates stable during annealing (De Hosson *et al.* 1999, Kooi *et al.* 1999). The same holds for indium. However, with gallium the size of the MnO precipitates decreases after dissolution of gallium by a factor of three to four, that is 200 ± 20 nm before, 64 ± 17 nm just after the introduction of gallium and 62 ± 6 nm after the additional week-long vacuum anneal.

A tentative explanation for the reduction in the precipitate size is the following. The introduction of gallium itself is not directly responsible for the shrinkage of the precipitates, because we determined that internally oxidized Cu–3 at.% Ga forms large Ga_2O_3 precipitates with a size between 200 and 350 nm. The strong reduction in the oxygen partial pressure that is accompanying the gallium introduction is probably more important. After internal oxidation the precipitates are oxygen terminated (Mader 1992, Backhaus-Ricoult 1999, Backhaus-Ricoult 2000, 2001) and, compared with the metal atoms with a high affinity for oxygen (manganese in this case), excess oxygen is present. After annealing in gallium vapour the oxide precipitates become metal terminated (Mader 1992, Backhaus-Ricoult 1999, Backhaus-Ricoult 2000, 2001) and excess metal is present in the precipitates, that is, the former

excess oxygen can now be used for the development of additional oxide. Simultaneously gallium is introduced which wants to form $Ga_xMn_yO_4$ precipitates (e.g. with $x = 1$ and $y = 2$). Then compared with the original MnO about the double of the amount of oxygen atoms needs to be present. That amount of excess oxygen is of course not available. Still as much as possible gallium and manganese atoms want to be oxidized; that is, as much as possible excess metal should be present in the precipitates. The only way to increase the amount of excess metal per precipitate is to decrease the size of the precipitates by which the surface area compared with the volume of the precipitate increases. This scenario works better for relatively small precipitates (e.g. with a size of 10 nm) where the surface area to volume is already large and the change from excess oxygen to excess metal implies a significant increase in the number of metal atoms that can become connected to the oxide. It is less effective for larger precipitates, but still the gallium atoms that can leave their unfavourable position in the copper matrix and can be incorporated in the oxide may outweigh the increase in interfacial area and thus interfacial energy. This reduction in precipitate size is of course aided if the interfacial energy of Cu–MnO is reduced with gallium introduction as appears to be the case.

§4. Conclusions

The present analysis shows that the earlier proposed approach for the analysis of Gibbsian segregation at heterointerfaces applying analytical TEM to edge-on oriented interfaces is a suitable method that allows the detection of a fraction of a monolayer coverage at a heterophase interface and the determination at which side of the heterophase interface segregation occurs. Segregation of gallium and indium and their competitive behaviour at parallel {111}-oriented Cu–MnO interfaces was analysed using three different sets of samples. In the first set that was obtained after dissolving about 3.8 at.% Ga in the copper matrix (1 week at 700°C) no significant segregation of gallium at the interfaces with the MnO precipitates was observed. In the second set produced after additionally dissolving about 3.4 at.% In in the copper matrix (an additional week at 750°C), weak segregation of gallium at the oxide side of the Cu–MnO interface was detected and relatively strong segregation of indium at the metal side of the interface was observed (17.6 at.% for the terminating monolayer of the copper matrix). In the third set that was obtained after annealing of the first set *in vacuo* for an additional week at 750°C (i.e. the same treatment as for introducing indium), strong segregation of gallium at the oxide side of the Cu–MnO interface was observed (about 14.3 at.% per monolayer for the first two monolayers of the oxide versus 2 at.% in the copper matrix). This leads to the conclusion that indium effectively blocks gallium segregation towards the oxide side of the interface. On the other hand, the presence of gallium does not influence the segregation of indium. Explanation for the gallium segregation at the oxide side is that a thin spinel-type $Ga_xMn_yO_4$ is formed that reduces the misfit at the metal–oxide interface. Full transformation of MnO precipitates into $Ga_xMn_yO_4$ is impossible because of the limited amount of oxygen present in the system. HRTEM images of the third set confirm that a thin outer layer (about 2 monolayers thick) of the oxide precipitates has a different structure with an intermediate misfit between copper and MnO that may lower the interfacial energy.

Acknowledgements

The work is part of the research programme of the Stichtung voor Fundamentele Onderzoek der Materie (Utrecht) and has been made possible by financial support from the Nederlandse Organisatie voor Wetenschappelijk Onderzoek (The Hague).

APPENDIX A

The fitting procedure to match the model curves with the XEDS results is performed numerically. As previously mentioned (see § 2) the assumed concentration profiles have the following definition (as an example, we show the result for enrichment in a single monolayer at the metal side of the interface):

$$\Omega_{\mathrm{A}}(n,x,y)=\begin{cases}1-x, & 0\leqslant n\leqslant 502,\\ 1-y, & 502\leqslant n\leqslant 522,\\ 0, & n>0,\end{cases}$$
$$\Omega_{\mathrm{B}}(n,x,y)=\begin{cases}x, & 0\leqslant n\leqslant 502,\\ y, & 502\leqslant n\leqslant 522,\\ 0, & n>522.\end{cases} \tag{A 1}$$

These concentration profiles $\Omega_{\mathrm{A}}(n,x,y)$and $\Omega_{\mathrm{B}}(n,x,y)$ are convoluted with the normalized Gaussian function mimicking the electron probe:

$$g(n)=A\exp\left(\frac{-n^2\ln(2)}{(50s)^2}\right). \tag{A 2}$$

The current variable n is assigned to the position across the interface, whereas by definition $502\leqslant n\leqslant 522$ represents a monolayer of 0.2 nm and the interface is located in between $n=522$ and $n=523$. s denotes the probe size (FWHM) of the electron beam in nanometres (see also Kooi *et al.* (2002)). The convolution is

$$C_{\mathrm{A}}(t,x,y)=\int_{-\infty}^{+\infty}\Omega_{\mathrm{A}}(n,x,y)g(n-t,s)\,\mathrm{d}n,$$
$$C_{\mathrm{B}}(t,x,y)=\int_{-\infty}^{+\infty}\Omega_{\mathrm{B}}(n,x,y)g(n-t,s)\,\mathrm{d}n. \tag{A 3}$$

The convoluted concentration profiles are shown in figures A 1 and A 2.

For the fitting procedure, it is not possible to use these convoluted concentration profiles directly as analytical functions (see figure 1), because they are multivalued functions. This means that there exists an ambiguous relation between the solvent–solute atomic concentrations (atomic percentages) with respect to the position t at the interface. This problem can be circumvented by fitting the convoluted concentration profile $C_{\mathrm{A}}(t,x,y)$ of solvent A with a unique analytical function. This solvent A profile can be non-ambiguously attributed to the position across the interface when fitting it with the following (Fermi) function:

$$f(t)=\frac{c100}{\exp\left[(t-a)/b^d\right]+1} \tag{A 4}$$

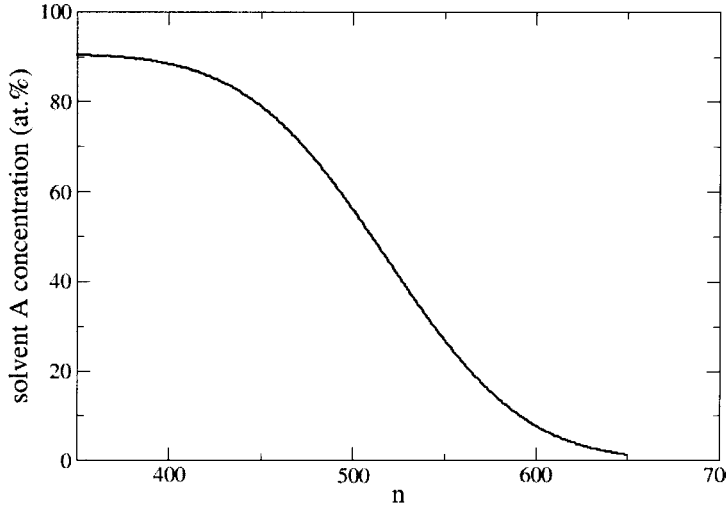

Figure A 1. Convolution of $\Omega_A(n, x, y)$ with the Gaussian function $g(n, s)$. The solvent concentration is 90 at.% at the metal side and 0 at.% at the oxide side of the interface. A probe size $s = 1.4$ nm was used (only the right-hand part, $t \geqslant 350$, of the function used for the fitting procedure is shown).

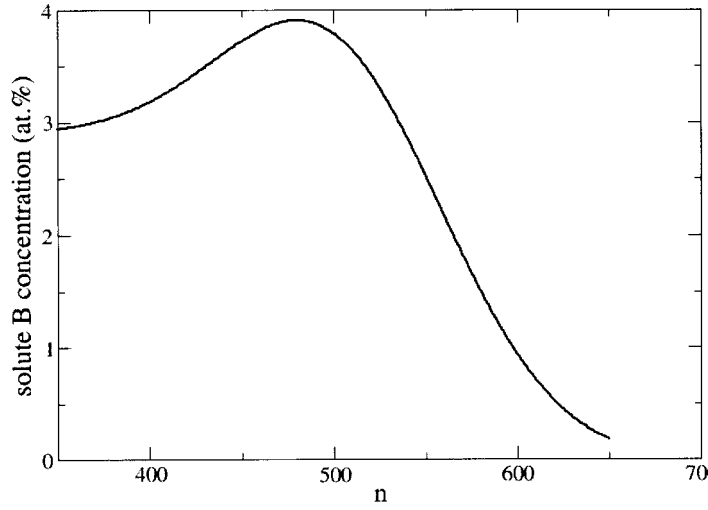

Figure A 2. Convolution of $\Omega_B(n, x, y)$ with the Gaussian function $g(n, s)$. The solute concentration B in the metal matrix is 2.9 at.% and 17.6 at.% in the last monolayer at the metal side of the interface. A probe size $s = 1.4$ nm was used (only the right-hand part, $t \geqslant 350$, of the function used for the fitting procedure is shown).

where a, b, c and d are fitting parameters. The attribution of the solvent concentration x_A as measured by XEDS to the position t can be made by setting $x_A = f(t)$ and solving equation (A 1) to $t_f(x_A)$:

$$t_f(x_A) = b^d \left[\ln \left(\frac{c100}{x_A} \right) - 1 \right] + a. \tag{A 5}$$

Now it is possible to match the assumed convoluted profile $C_B(t_f, x, y)$ of solute B and the XEDS measured segregation y_B across the interface by calculating the minimum of the least square function:

$$\Gamma = \left(\sum_i [y_{B_i} - C_{B_i}(t_f, x, y)]^2 \right)^{1/2}, \tag{A 6}$$

where the summation runs over all the measurements. For segregation, the concentration y_B in the outermost monolayer of the metal at the interface depends on the convolution profile of solvent A (via t_f) and therefore influences the fitting parameters a, b, c and d. The solute concentration x in solvent A and the size of the electron beam are kept constant during fitting procedures. This drawback in the fitting procedure is not significant because, after each procedure performed, the obtained value y can used as a new input variable in the assumed convoluted profile of solvent A. After three iterations by using y as a new input parameter the matched segregation y_B converges to a fixed value. This fitting procedure can be performed analogously to quantify segregation in the first (two) monolayer(s) at the oxide side of the interface by redefining the rectangular functions in equation (A 1).

References

Backhaus-Ricoult, M., 2000, *Acta mater.*, **48**, 4365; 2001, *ibid.*, **49**, 1747.

Backhaus-Ricoult, M., and Laurent, S., 1999, *Mater. Sci. Forum*, **294–296**, 173.

Baker, H., 1992, *ASM Handbook*, Vol. 3, *Alloy Phase Diagrams* (Materials Park, Ohio: American Society for Metals).

Cliff, G., and Lorimer, G. W., 1975, *J. Microsc.*, **103**, 203.

De Hosson, J. Th. M., Groen, H. B., Kooi, B. J., and Vitek, V., 1999, *Acta mater.*, **47**, 4077.

EDAX, 2000, *EDAX Phoenix Software, TEM Quant Materials, Version 3.2* (Mahwah, New Jersey: EDAX Inc.).

Groen, H. B., Kooi, B. J., Vellinga, W. P., and De Hosson , J. Th. M., 1999, *Phil. Mag.* A, **79**, 2083.

Hayes, P., and Grieveson, P., 1995, *Metal Sci.*, **9**, 332.

Joint Committee for Powder Diffraction Standards, 1992, Powder Diffraction File (Swarthmore, Pennsylvania: International Centre for Diffraction Data), card 36-0181.

Johnson, W. C., and Blakely, J. M. (editors), 1979, *Interfacial Segregation* (Metals Park, Ohio: American Society for Metals).

Kooi, B. J., Groen, H. B., and De Hosson, J. Th. M., 1998, *Acta mater.*, **46**, 111.

Kooi, B. J., Westers, A. R.,Vreeling, J. A., van Agterveld, D. T. L., and De Hosson, J. Th. M., 1999, *Mater. Sci. Forum*, **294–296**, 255.

Kooi, B. J., Wouters, O., and De Hosson, J. Th. M., 2002, *Acta mater.*, **50**, 223

Mader, W., 1992, *Z. Metallk.*, **83**, 7.

Pipel, E., Woltersdorf, J., Gegner, J., and Kirchheim, R., 2000, *Acta mater.*, **48**, 2571.

Reed, S. J. B., 1982, *Ultramicroscopy*, **7**, 405.

Rhines, F. N., and Grobe, A. H., 1942, *Trans. AIME*, **147**, 318.

Rühle, M., 1997, *Handbook of Microscopy; Applications*, edited by S. Amelinckx, D. van Dyck, J. van Landuyt and G. Van Tendeloo (Weinheim: VCH), pp. 285–288.

Sebastian, J. T., Rüsing, J., Hellman, O. C., Seidman, D. N., Vriesendorp, W., Kooi, B. J., and De Hosson, J., Th., M., 2001, *Ultramicroscopy*, **89**, 203.

Shashkov, D. A., 1997, PhD Thesis, Northwestern University, Evanston, Illinois, USA.

Shashkov, D. A., Muller, D. A., and Seidman, D. N., 1999, *Acta. mater.*, **47**, 3953.

Vriesendorp, W., Kooi, B. J., and De Hosson, J. Th. M., 2001, *Scripta Mater.*, **45**, 169.